Rolling Bearing Feature Frequency Extraction using Extreme Average Envelope Decomposition

SHI Kunju, LIU Shulin*, JIANG Chao, and ZHANG Hongli

School of Mechatronics Engineering and Automation, Shanghai University, Shanghai 20072, China

Abstract: The vibration signal contains a wealth of sensitive information which reflects the running status of the equipment. It is one of the most important steps for precise diagnosis to decompose the signal and extracts the effective information properly. The traditional classical adaptive signal decomposition method, such as EMD, exists the problems of mode mixing, low decomposition accuracy etc. Aiming at those problems, EAED(extreme average envelope decomposition) method is presented based on EMD. EAED method has three advantages. Firstly, it is completed through midpoint envelopment method rather than using maximum and minimum envelopment respectively as used in EMD. Therefore, the average variability of the signal can be described accurately. Secondly, in order to reduce the envelope errors during the signal decomposition, replacing two envelopes with one envelope strategy is presented. Thirdly, the similar triangle principle is utilized to calculate the time of extreme average points accurately. Thus, the influence of sampling frequency on the calculation results can be significantly reduced. Experimental results show that EAED could separate out single frequency components from a complex signal gradually. EAED could not only isolate three kinds of typical bearing fault characteristic of vibration frequency components but also has fewer decomposition layers. EAED replaces quadratic enveloping to an envelope which ensuring to isolate the fault characteristic frequency under the condition of less decomposition layers. Therefore, the precision of signal decomposition is improved.

Keywords: adaptive signal decomposition, extreme average envelope decomposition, EMD, fault diagnosis

1 Introduction

Mechanical systems are developing towards large-scale, high speed and good precision，so the composition of equipment is becoming more and more complex. The connections among mechanical parts are increasingly close. The failure of any mechanical part will cause the disruption of production and even cause a greater loss. How to find the fault information that contains the equipment running status timely and effectively is one of the key steps to the right decisions. Because the fault signal usually has the characteristics of nonlinear, non-Gaussian and non-stationary, traditional signal analysis methods, for example, short-time Fourier transform and wavelet transform based on basis function similarity matching principle, are hard to describe the real world signal through limited basis function. Empirical mode decomposition(EMD) is a data driven adaptive signal decomposition method that decomposes the signal according to its own characteristics. EMD decomposes complex non-stationary signal into a series of approximately single component signal by which the useful sensitive information can be isolated.

EMD method has been proposed by HUANG, et al[1] since 1998. Then it has been widely used in signal de-noising[2–3], fault diagnosis[4–7], biomedical analysis[8–10] etc. and has achieved great success. However, further applications are limited owing to the drawbacks of end effect, mode mixing and other disadvantages. Many experts and scholars were dedicated to the research on EMD method. A series of improvement methods have been put forward. For example, based on the statistical properties of white noise, WU and HUANG[11] proposed a new EEMD method to overcome the mode mixing problem; and then aiming at multidimensional data(such as images or solid with variable density) analysis, WU and HUANG[12] proposed a multi-dimensional ensemble empirical mode decomposition(MEEMD) method which can be extended to any higher dimensional temporal-spatial data. BAGHERZADEH, et al[13], introduced the variable-span smoothing sifting for EMD and extracted the local mean of the signal at each point by applying some smoothing filters to its adjacent data points with the advantages of direct, local, and online. Based on EMD, LI, et al[14], proposed an optimized rational Hermite interpolation method and then applied the method to automatically select the suitable shape controlling parameter in each sifting process, which can improve the reliability and accuracy significantly.

In the area of mechanical fault diagnosis, EMD has been used in predicting residual fatigue life of materials and detecting the faults of machinery components, such as rolling element bearings, gears and rotors. Some scholars combined EMD directly with other methods to form a new machinery fault diagnosis method. For example, ALI, et al[15], combined EMD energy entropy and artificial neural network for rolling element bearing fault diagnosis, and then presented a mathematical analysis method to select the most significant intrinsic mode functions(IMFs). GEORGOULAS, et al[16], proposed a novel approach based on the complex empirical mode decomposition combined EMD and Markov models, which applied to the diagnosis of rotor asymmetries in asynchronous machines. EMD-ICA method was proposed by ZHANG, et al[17]. Rolling bearing vibration signals were decomposed using EMD method and then based on mutual correlation criterion and FastICA method, source signals and noise signals were separated successfully. LIU, et al[18], integrated EMD and the LS-SVM to develop a novel fault diagnosis method of rotary machines.

Several researchers improved EMD and make EMD more suitable for machinery diagnosis. For example, using EMD, UX, et al[19], decomposed ball bearings vibration signals and root mean square of intrinsic mode function involving fault characteristic frequency has a consistent trend with the diameter of flaws, then proposed two improved Paris models to find out a characteristic value of vibration signals monitored in the process of machine operation to describe the severity of the flaw in time domain and predict fatigue life. In order to make sure rolling element bearings vibration signal properly de-noised, VAN, et al[20], hybrid technique of non-local means de-noising and EMD, which can successfully extract impulsive features from noise signals. SUI, et al[21], proposed an adaptive envelope spectrum technique based on EMD, and applied the method to different bearing conditions. LU, et al[22], employed EMD to decompose a vibration signal into intrinsic mode functions (IMFs) and then used modified genetic algorithm to select dominant features for SVM to classify different fault patterns. ZHAO, et al[23], proposed an IMF-based adaptive envelope order analysis for bearing fault detection under harsh condition(e.g., time-varying speed and load, large shocks).

Scholars also use improved EMD version for machinery fault diagnosis, such as EEMD, CEEMD and LMD etc. to achieve machinery diagnosis. Based on EEMD and SVM ZHANG, et al[24], presented a novel procedure for multi-fault diagnosis of rolling elements. An adaptively fast EEMD method combined with complementary EEMD was proposed by XUE, et al[25], to solve the problems of high computational cost, critical parameters determination, and the contamination of the residue noise in the signal reconstruction. In order to detect partially broken of rotor bars, GARCIA-PEREZ, et al[26], studied and evaluated the condition monitoring method based on CEEMD, and finally found CEEMD had the advantage of being an online diagnosis method, which does not require knowing a priori motor current of the healthy condition. FENG, et al[27], diagnosed planetary gear box by joint application of the LMD and Fourier transform.

The above studies show that EMD and its improved methods can solve practical problems. However, the essence of these methods separates components by double enveloping tactics, which increase the envelope error.

In order to improve the accuracy of the decomposition, a method named EAED(extreme average envelope decomposition) is proposed in this paper. EAED method provides an effective way to adaptively decompose the raw vibration signal into a series of components with different frequency bands properly.

The rest of this article is organized as follows. The proposed EAED technique is analysised and discussed in section 2. The effectiveness of the proposed technique is tested by simulation signals in section 3. Vibration signals of rolling bearing are analyzed by EAED and EMD method to verify the new method in section 4. Some concluding remarks are summarized in section 5.

2 Analysis of Extreme Average Envelope Decomposition

The essence of extreme average envelope decomposition scheme is to iteratively subtract midpoint envelope data from original signal. Section 2.1 analyses two envelops strategies and finds that the middle envelope method can reveal the frequency component more precisely. The middle envelope data have the same frequency with the low frequency components in a signal but the former has a smaller amplitude, which is discussed in section 2.2. For this reason, we took iterative strategy to remove the low frequency information and separate various frequency components. Section 2.3 gives a method to determine middle point location by using similar triangle principle. Section 2.4 states EAED algorithm steps. Section 2.5 studies the anti-noise ability in EAED and EMD.

2.1 Comparison of two envelop methods in EAED and EMD

The key part of EMD is average upper and lower envelope. We obtained the envelope curve by calculating the mean value of both local maximum point and local minimum point. The EAED envelope curve is formed by three order spline interpolation based on the local mean value namely middle envelope method.

We took two component signals(Fig. 1 thick curve) $x(t) = \sin(2\pi \times 20t) + \sin(2\pi \times 80t)$ for example to analyze the characteristics of two envelope methods. The dashed curve in Fig. 1 is the result of middle envelope method used by EAED. The thin curve in Fig. 1 is the result of average upper and lower envelope method used by EMD. The envelope method used in EAED can show more detail

information. The middle envelope curve has the same frequency of the raw signal, which is not reflected in average upper and lower envelope method.
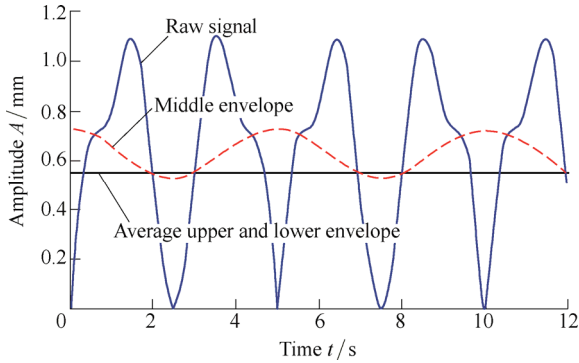

Fig. 1.   Comparison of two envelope methods

2.2   Relations between middle point and low frequency components

The signal $x(t) = \sin(2\pi \times 100t) + \sin(2\pi \times 200t)$ was chosen for example. In Fig. 2, the thick curve represents the original vibration signal. The dashed curve is a lower frequency component of the original signal and the thin curve is the result of three order spline interpolation based on the original signal middle points. Fig. 2 illustrations that the low frequency components and cubic spline middle point fitting curve are intersected at a point，such as point a, b and c. As for the low frequency signal and cubic spline curve, a period can be achieved from point a to point c. They have the same frequency but different amplitude. The midpoint which implicated the low frequency information is a signal intrinsic characteristic. So in section 2.3, in order to obtain the low frequency component information of the original signal, the algorithm needs to get the mid-range of the signal every time.
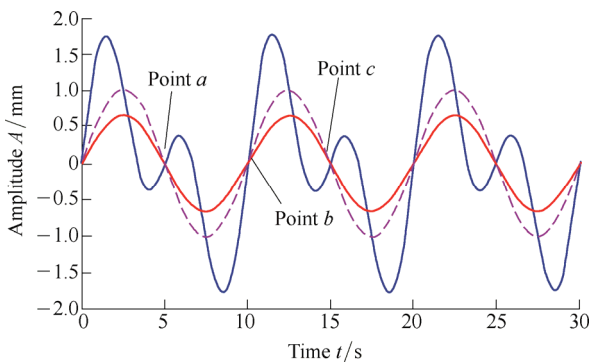

Fig. 2.   Relations among the original signal, low frequency signal and cubic spline curve

2.3   Time determination of middle point

It is one of the critical steps to determine the location of the middle point. Generally cubic spline middle points are not sampling points because of the limitation of the sampling frequency(Fig. 3). We used similar triangle principle to determine the time of the midpoint value.
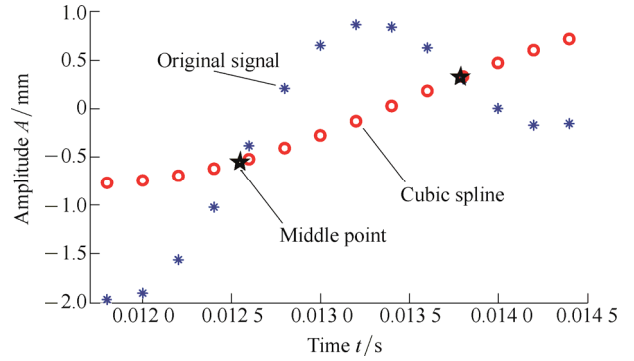

Fig. 3.   Location of middle point and cubic spline curve

Suppose a and b are sampling points of the original signal, t_1 and t_2 are the times of a and b, respectively. t_3 is the time of c as shown in Fig. 4. Using similar triangle principle, we have

$$\frac{t_3 - t_1}{val(c) - val(a)} = \frac{t_2 - t_1}{val(b) - val(a)}, \tag{1}$$

then t_3 can be rewritten as

$$t_3 = \frac{val(c) - val(a)}{val(b) - val(a)} \times (t_2 - t_1) + t_1. \tag{2}$$
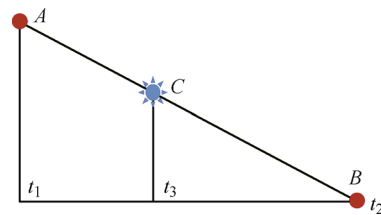

Fig. 4.   Relations between sampling points and middle point

The discrete form of Eq. (2) is

$$k = \frac{val(mid(i)) - val(x(j))}{val(x(j+1)) - val(x(j))} \times (j+1) + j =$$

$$\frac{val(mid(i)) - val(x(j))}{val(x(j+1)) - val(x(j))} + j. \tag{3}$$

$val(*)$ represents the value of $*$th point. For a signal x, $mid(i)$ represents the ith middle point, $x(j+1)$ and $x(j)$ are the nearest point of $mid(i)$. k is the time of $mid(i)$ in signal x.

2.4   Algorithm steps of EAED method

The main idea of EAED algorithm is to extract particular frequency information using midpoint, and then accumulate the particular frequency information until the particular frequency information in the original signal frequency component is smaller than a certain threshold. We choose the accumulation of signal components as a component signal. Repeat the above process for the signals that the particular frequencies have been removed and the iteration should be stopped until mid-range less than two.

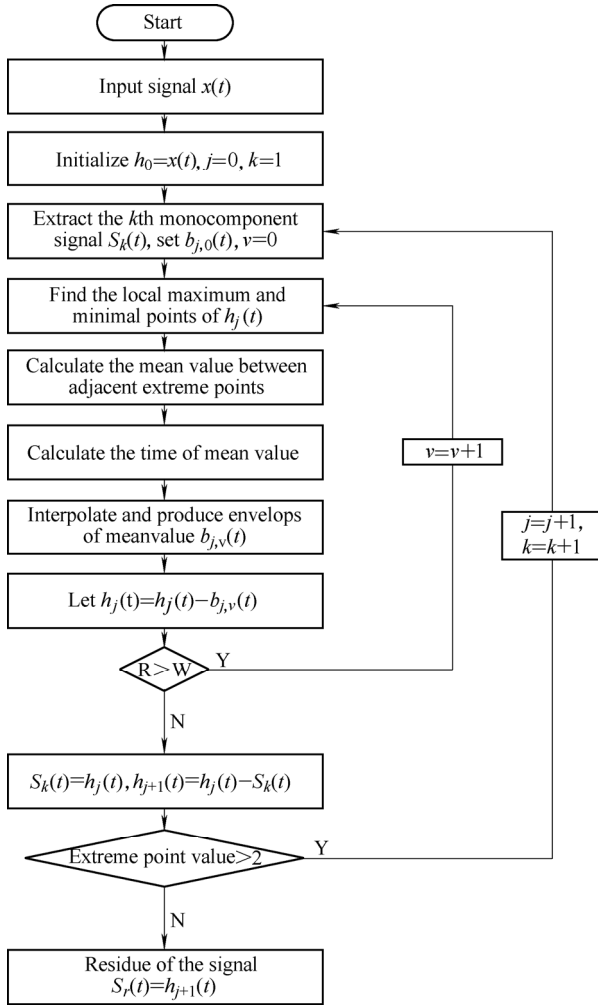In summary, we state EAED as the following algorithm (Fig. 5 is the flow chart of EAED algorithm).

Fig. 5.   Flow chart of EAED algorithm

(1) Initialize: $h_0=x(t)$, $j=0$, $k=1$.

(2) Extract the kth monocomponent signal $S_k(t)$ and set $b_{j,0}=0$, $v=0$.

(a) Suppose $h_j(t)$ has p local maximum points and q local minimal points. Find out all local maximum $pmax_{j,p}$ and $pmin_{j,q}$ points of $h_j(t)$.

(b) Find out the corresponding time $tmax_{j,p}$ and $tmin_{j,q}$ of $pmax_{j,p}$ and $pmin_{j,q}$.

(c) $tmax_{j,p}$ and $tmin_{j,q}$ divide $h_j(t)$ into $(p+q-1)$ intervals. Suppose the ith interval has n sample points and calculate the average of $S_j(t)$ within every interval $m_{j,i}$ by Eq. (4):

$$m_{j,i} = \frac{\sum_{l=1}^{n} h_{j,i}(l)}{n}. \tag{4}$$

(d) The corresponding time $t_{a,j}$ of $m_{j,i}$ is calculated by using Eq. (3).

(e) Interpolate and produce envelops of all adjacent average points using $m_{j,i}$ and $t_{a,j}$, and then obtain a function $b_{j,v}(t)$.

(f) Let $h_j(t)=h_j(t)-b_{j,v}(t)$, $v=v+1$.

(g) R is calculated by using Eq. (5). If $R>W$, go to step (a). Else set $S_k(t)=h_j(t)$.

$$R = \frac{(b_j(t))_{max} - (b_j(t))_{min}}{(h_j(t))_{max} - (h_j(t))_{min}}. \tag{5}$$

(3) $h_{j+1}(t)=h_j(t)-S_k(t)$, $k=k+1$. If h_{j+1} still has at least 2 extreme points the next step then go to step (2) with $j=j+1$. If not, the decomposition process is finished and we set $S_r(t)=h_{j+1}(t)$. $S_r(t)$ is the residue.

2.5   Analysis of anti-noise ability in EAED and EMD

The signal often contains noise. Adaptive signal decomposition method, such as EAED and EMD, decomposes the signal from high frequency to low frequency. The noise signal can be decomposed in previous several layers. In order to identify the degree that the noise can affect the decomposition results, the signal $x(t) = \sin(2\pi \times 100t) + \sin(2\pi \times 200t)$ was added noise and then calculate the similarity degree between the first decomposition layer and the noise signal. The correlation coefficient was selected to express the similarity degree quantitatively. The calculation results are showed in Fig. 6. Value of correlation coefficient is near 0.87(EAED method) and 0.72(EMD method), respectively. In addition, the correlation coefficient fluctuations are small.
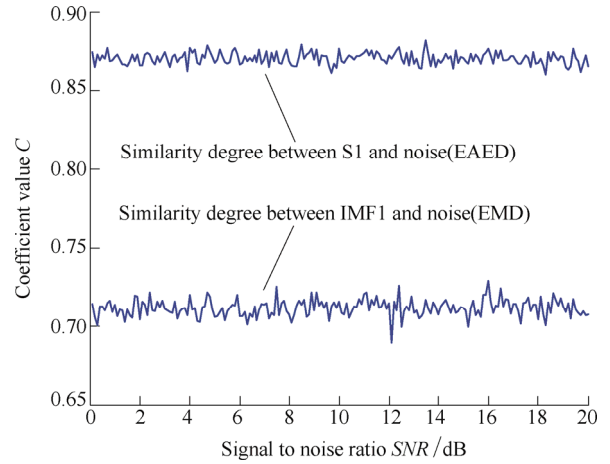

Fig. 6.   Similarity degree between the first
decomposition layer and the noise signal

3   Simulation and Discussion

In this section, we choose typical signals to conduct EAED and EMD. As compared with EMD method, the decomposition ability of the method was studied.

3.1   Decomposition of signal containing noise

As for the signal containing noise, adaptive decomposition method can separate the noise signal. $x(t)$ is a compound signal containing noise, $x(t)=x_1(t)+x_2(t)+x_3(t)$(Fig. 7). $x_1(t)$ is stochastic noise. $x_2(t) = \cos(2\pi t)$. $x_3(t) = 0.5\cos(8\pi t)$. EAED and EMD decomposition are

implemented respectively and the results are shown in Fig. 8 and Fig. 9. EAED method can decompose the noise into two components. S3 and S4 components are high frequency $x_2(t)$ and low frequency components $x_3(t)$ of the original signal, respectively. S5 is the residual component. EMD method decomposes the noise signal into four components. The IMF5, IMF6 components are the original signal of high frequency $x_2(t)$ and low frequency components $x_3(t)$ respectively. The number of component layers decomposed by EAED method is relatively small and decomposition results have less distortion.
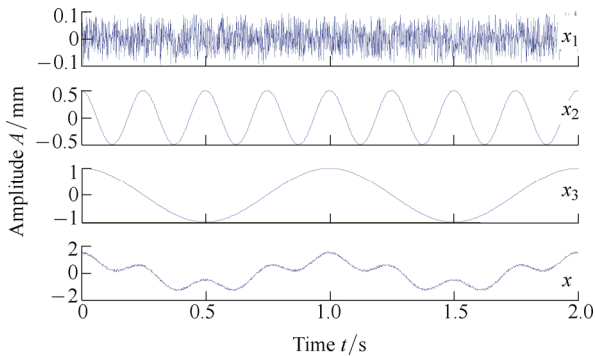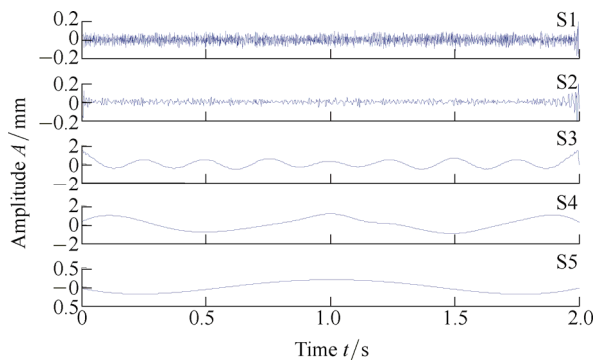

Fig. 7. Signal containing noise

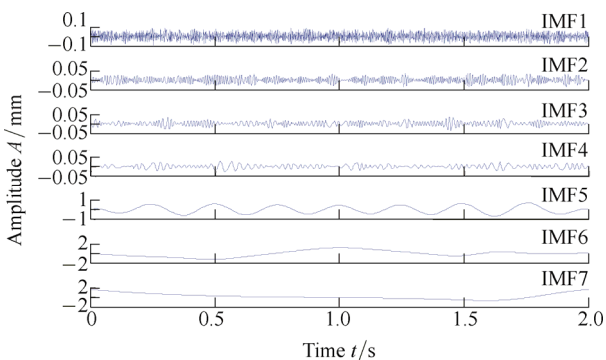Fig. 8. Decomposition of signal containing noise based on EAED

Fig. 9. IMF components of signal containing noise

3.2 Multi-component frequency signal decomposition

As for the signal containing multi-frequency components $x(t)=x_1(t)+x_2(t)+x_3(t)$. $x(t)$ consists of three different frequency components(Fig. 10). $x_1(t)=0.5\cos(4\pi t)$. $x_2(t)=5\sin(20\pi t)$ $x_3(t)=20\cos(70\pi t)$. With EAED and EMD method, the results are presented in Fig. 11 and Fig.

12. The former three components decomposed by EAED method can better recover the three components of the raw signal. The EMD method has a large distortion and decomposes many components.
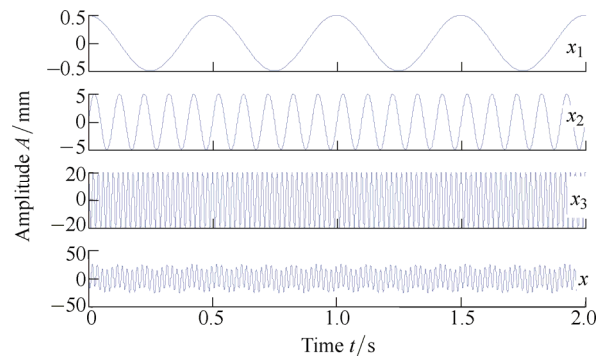

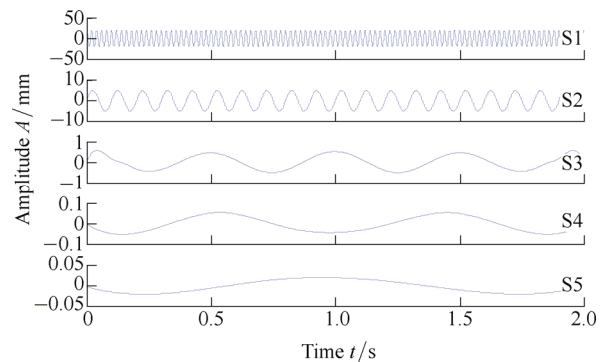Fig. 10. Multi-component frequency signal

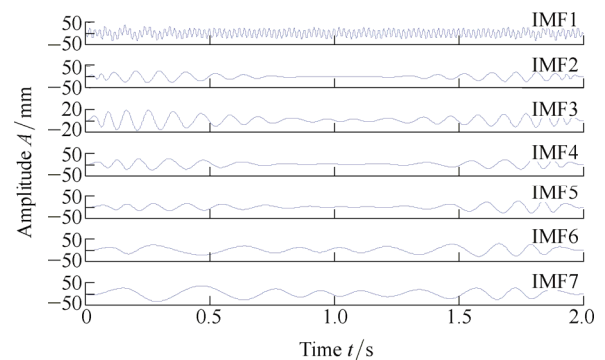Fig. 11. Decomposition of multi-component frequency signal by EAED

Fig. 12. IMF components of multi-component frequency signal

4 EAED in Bearing Fault Diagnosis

In order to verify the effectiveness of the EAED method, EAED and EMD method were used respectively to decompose vibration signals of inner race fault in rolling bearing. The test data is from the data center of Case Western Reserve University bearing drive end bearing vibration. The specific bearing parameters are shown in Table 1. The vibration signals were collected by using accelerometers attached to the housing of induction motor near to the test bearing with the sampling frequency f_s of 12 000 Hz. The rotating speed of the rolling bearing was 1750 r/min. Based on the rotating speed, the rotating

frequency of the rolling bearing f_R is 29.17 Hz.

Parameter	Value
Number of bearing elements z	9
Bearing elements diameter d/mm	7.94
Bearing medium diameter D/mm	39
Contact angle α/(°)	90

According to the data in Table 1 and Eq. (6), the characteristic frequency with inner race failure is calculated to be $f_{IR}=157.94$ Hz:

$$f_{IR} = \frac{1}{2} Z \left(1 + \frac{d}{D} \cos \alpha\right) f_0 = 157.94 \text{ Hz.} \tag{6}$$

Fig. 13 and Fig. 14 are a part of EAED and EMD decomposition results of inner race fault vibration data respectively. It can be observed that the layer number of EAED decomposition is fewer. Simultaneously, the result of EAED decomposition preserves impact characteristics of the signal more accurately.
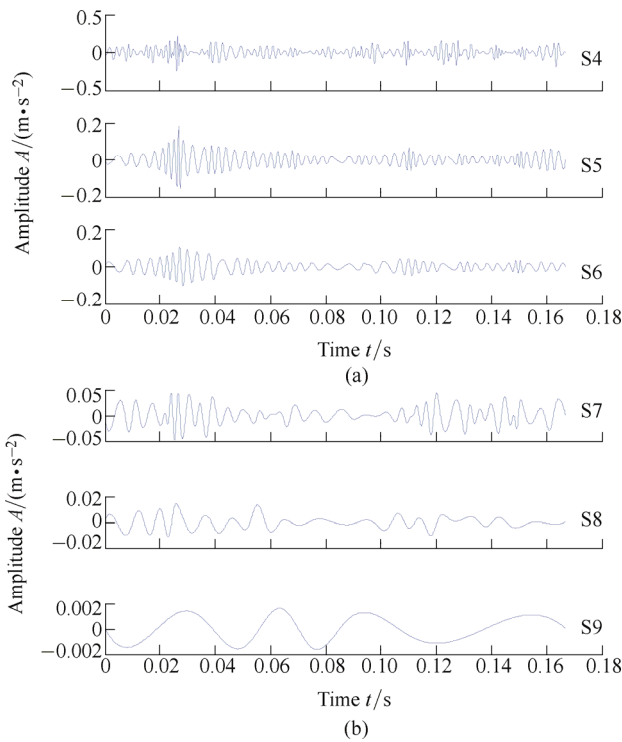

Fig. 13.   Vibration signal of inner race fault
after EAED decomposition

The Fourier transform was performed on each layer data respectively. Analysis results are shown in Fig. 15 and Fig. 16. The main frequency of each component is shown in Table 2 and Table 3, respectively. It can be seen that S7, S5 and S4 respectively correspond to the inner race fault frequency f_{IR}, its 2nd harmonic frequency triple, and its 3rd harmonic frequency as displayed in Fig. 15. S9 and S8 correspond to rolling bearing rotating frequency f_R and its 4th harmonic frequency after EAED decomposition. Only

IMF11 component corresponds to rolling bearing rotating frequency f_R and other sensitive frequency components are difficult to find.
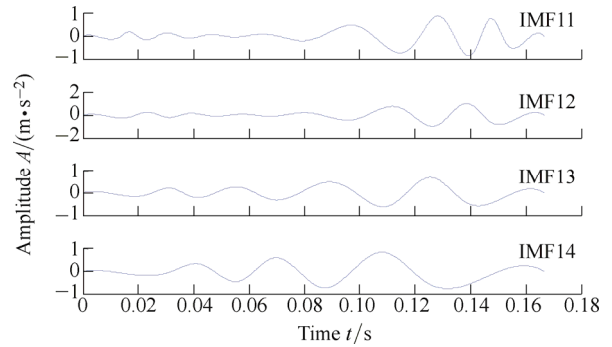

Fig. 14.   Vibration signal of inner race fault
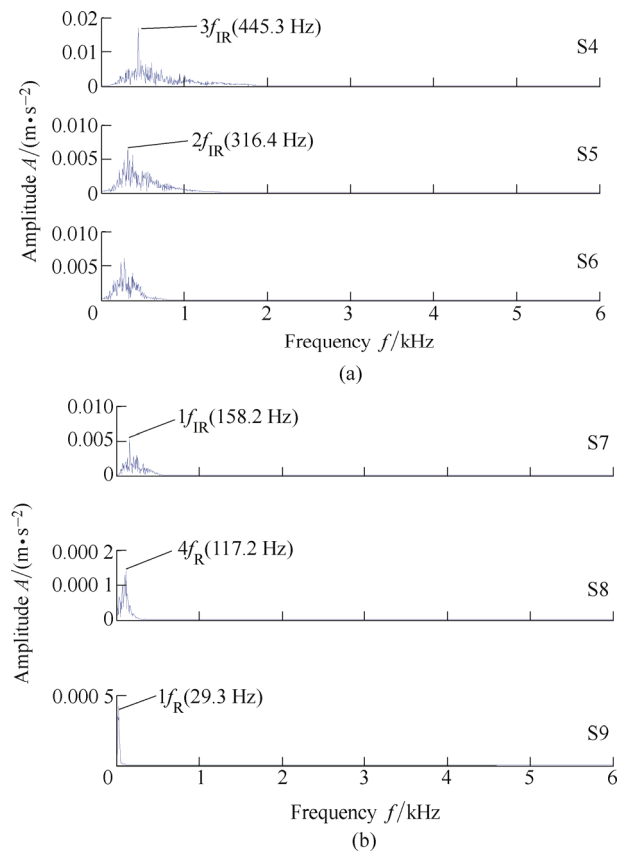after EMD decomposition

Fig. 15.   Spectrum analysis of fault vibration signal
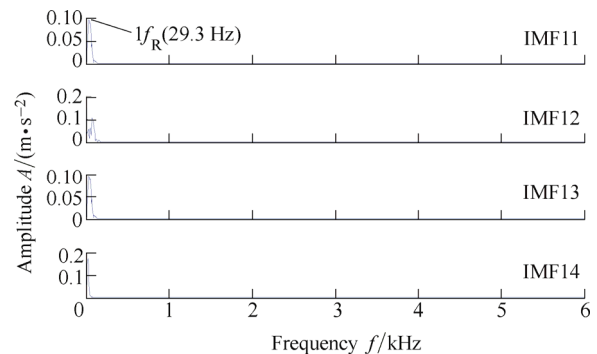from inner race after EAED decomposition

Fig. 16.   Spectrum analysis of inner race fault vibration
signal after EMD decomposition

Table 2. Main frequency components of inner race fault vibration signal after EAED decomposition

EAED component	Frequency f/Hz	EAED component	Frequency f/Hz
S1	2813	S7	158.2
S2	2338	S8	117.2
S3	603.5	S9	29.3
S4	445.3	S10	17.58
S5	316.4	S11	5.859
S6	275.4	S12	5.85

Table 3. Main frequency components of inner race fault vibration signal after EMD decomposition

EMD component	Frequency f/Hz	EMD component	Frequency f/Hz
IMF1	2813	IMF10	76.17
IMF2	1922	IMF11	29.3
IMF3	720	IMF12	70.31
IMF4	603	IMF13	41.02
IMF5	445	IMF14	23.44
IMF6	287	IMF15	23.44
IMF7	216	IMF16	17.58
IMF8	76.17	IMF17	11.72
IMF9	93.75	IMF18	11.72

The EAED and EMD analysis results of bearing vibration signals show that these two methods can adaptive decompose the raw signal from high frequency to low frequency. EAED analysis results not only can find more physical meaning component but also can separate the high frequency noise, bearing fault signal and the bearing rotation signal properly. In addition, compared with EMD, EAED can obtain fewer decomposed layers.

5 Conclusions

(1) A method of adaptive signal decomposition named EAED is presented. In order to find local real information of raw signal properly, EAED uses the arithmetic mean of maximum and minimum rather than the average of upper and lower envelope. EAED method adopts a strategy that replaces two envelopes with one envelope, which reduced the envelope errors of the signal decomposition. Using the similar triangle principle, we can accurately calculate the location according to the middle point, which improved the precision of decomposition. Theoretical analysis proves the validity of EAED method.

(2) Typical simulation signals have been decomposed, and the result shows that EAED method can separate the complex signal, restore the different frequency signal and noise signal. The vibration signal of rolling bearing has been tested by EAED and EMD method. The results demonstrated that signals decomposed by EAED have a clear physical meaning and can clearly find the characteristic frequency of the bearing fault and bearing rotation frequency after Fourier transformation. Experimental results indicate that the signal decomposed by EAED method contains more detailed information and can provide a new way for signal analysis.

References

[1] HUANG N E, SHEN Z, LONG S R, et al. The empirical mode decomposition and the Hilbert spectrum for nonlinear and non-stationary time series analysis[J] *Proceedings of the Royal Society of London A: Mathematical, Physical and Engineering Sciences. The Royal Society*, 1998, 454(1971): 903–995.

[2] SHUKLA S, MISHRA S, SINGH B. Power quality event classification under noisy conditions using EMD-based de-noising techniques[J]. *Industrial Informatics IEEE Transactions on*, 2014, 10(2): 1044–1054.

[3] YANG G, LIU Y, WANG Y, et al. EMD interval thresholding denoising based on similarity measure to select relevant modes[J]. *Signal Processing*, 2015, 109: 95–109.

[4] GUO W, PETER W T. A novel signal compression method based on optimal ensemble empirical mode decomposition for bearing vibration signals[J]. *Journal of Sound and Vibration*, 2013, 332(2): 423–441.

[5] GUO C, AL-SHUDEIFAT M A, YAN J, et al. Application of empirical mode decomposition to a jeffcott rotor with a breathing crack[J]. *Journal of Sound and Vibration*, 2013, 332(16): 3881–3892.

[6] WANG C, GAN M, ZHU C. Non-negative EMD manifold for feature extraction in machinery fault diagnosis[J]. *Measurement*, 2015, 70: 188–202.

[7] GUO W, PETER W T. Enhancing the ability of ensemble empirical mode decomposition in machine fault diagnosis[C]//*Prognostics and Health Management Conference*, Portland, USA, October 10–14, 2010: 1–7.

[8] COLOMINAS M A, SCHLOTTHAUER G, TORRES M E. Improved complete ensemble EMD: a suitable tool for biomedical signal processing[J]. *Biomedical Signal Processing and Control*, 2014, 14: 19–29.

[9] CHANG C C, KAO S C, HSIAO T C, et al. Assessment of autonomic nervous system by using empirical mode decomposition based reflection wave analysis during non-stationary conditions[J]. *Physiological Measurement*, 2014, 35(9): 1873–1883.

[10] GAO L, ZHANG Y, LIN W, et al. A novel quadrature clutter rejection approach based on the multivariate empirical mode decomposition for bidirectional Doppler ultrasound signals[J]. *Biomedical Signal Processing and Control*, 2014, 13: 31–40.

[11] WU Z, HUANG N E. Ensemble empirical mode decomposition: a noise-assisted data analysis method[J]. *Advances in Adaptive Data Analysis*, 2009, 1(1): 1–41.

[12] WU Z, HUANG N E, CHEN X. The multi-dimensional ensemble empirical mode decomposition method[J]. *Advances in Adaptive Data Analysis*, 2009, 1(3): 339–372.

[13] BAGHERZADEH S A, SABZEHPARVAR M. A local and online sifting process for the empirical mode decomposition and its application in aircraft damage detection[J]. *Mechanical Systems and Signal Processing*, 2015, 54: 68–83.

[14] LI Y, XU M, WEI Y, et al. An improvement EMD method based on the optimized rational Hermite interpolation approach and its application to gear fault diagnosis[J]. *Measurement*, 2015, 63: 330–345.

[15] ALI J B, FNAIECH N, SAIDI L, et al. Application of empirical mode decomposition and artificial neural network for automatic bearing fault diagnosis based on vibration signals[J]. *Applied Acoustics*, 2015, 89: 16–27.

[16] GEORGOULAS G, TSOUMAS I P, ANTONINO-DAVIU J A, et al. Automatic pattern identification based on the complex empirical mode decomposition of the startup current for the diagnosis of rotor asymmetries in asynchronous machines[J]. *Industrial Electronics, IEEE Transactions on*, 2014, 61(9): 4937–4946.

[17] ZHANG J H, LI L J, MA W P, et al. Application of EMD-ICA to fault diagnosis of rolling bearings[J]. *Chinese Journal of Mechanical Engineering*, 2013, 24(11): 1468–1472.

[18] LIU X, BO L, LUO H, et al. Bearing faults diagnostics based on hybrid LS-SVM and EMD method[J]. *Measurement*, 2015, 59: 145–166.

[19] XU D, ZHU Q, CHEN X, et al. Residual fatigue life prediction of ball bearings based on Paris law and RMS[J]. *Chinese Journal of Mechanical Engineering*, 2012, 25(2): 320–327.

[20] VAN M, KANG H J, SHIN K S. Rolling element bearing fault diagnosis based on non-local means de-noising and empirical mode decomposition[J]. *IET Science, Measurement & Technology*, 2014, 8(6): 571–578.

[21] SUI W, OSMAN S, WANG W. An adaptive envelope spectrum technique for bearing fault detection[J]. *Measurement Science and Technology*, 2014, 25(9): 1–9.

[22] LU L, YAN J, SILVA C W. Dominant feature selection for the fault diagnosis of rotary machines using modified genetic algorithm and empirical mode decomposition[J]. *Journal of Sound and Vibration*, 2015, 344: 464–483.

[23] ZHAO M, LIN J, XU X, et al. Multi-fault detection of rolling element bearings under harsh working condition using IMF-based adaptive envelope order analysis[J]. *Sensors*, 2014, 14(11): 20320–20346.

[24] ZHANG X, ZHOU J. Multi-fault diagnosis for rolling element bearings based on ensemble empirical mode decomposition and optimized support vector machines[J]. *Mechanical Systems and Signal Processing*, 2013, 41(1): 127–140.

[25] XUE X, ZHOU J, XU Y, et al. An adaptively fast ensemble empirical mode decomposition method and its applications to rolling element bearing fault diagnosis[J]. *Mechanical Systems and Signal Processing*, 2015, 62: 444–459.

[26] GARCIA-PEREZ A, IBARRA-MANZANO O, ROMERO-TRONCOSO R J. Analysis of partially broken rotor bar by using a novel empirical mode decomposition method[C]//*The 40th Annual Conference of the IEEE Industrial Electronics Society*(*IECON-2014*). Dallas, USA, October–November, 2014: 3403–3408.

[27] FENG Z, ZUO M J, QU J, et al. Joint amplitude and frequency demodulation analysis based on local mean decomposition for fault diagnosis of planetary gearboxes[J]. *Mechanical Systems and Signal Processing*, 2013, 40(1): 56–75.

Biographical notes

SHI Kunju, born in 1984, is currently a PhD candidate at *School of Mechatronics Engineering and Automation, Shanghai University, China*. His research interests include signal processing and fault diagnosis.
Tel: +86-15921838572; E-mail: shikunjv@sina.cn

LIU Shulin, born in 1963, is currently a professor and a doctoral supervisor at *School of Mechatronics Engineering and Automation, Shanghai University, China*. He received his PhD degree from *Harbin Institute of Technology, China*, in 2003. His major research direction is complex equipment fault diagnosis.
Tel: +86-21-56331523; E-mail:lsl346@shu.edu.cn

JIANG Chao, born in 1987, is currently a PhD candidate at *School of Mechatronics Engineering and Automation, Shanghai University, China*. His research interests include the fault diagnosis method based on signal processing.
E-mail: jc31@163.com

ZHANG Hongli, born in 1985, is currently a postdoctor at *Shanghai Institute of Applied Mathematics and Mechanics, Shanghai University, China*. He received his PhD degree from *Shanghai University, China*, in 2014. His research interests include intelligent fault diagnosis and pattern recognition.
E-mail:zhang40941@126.com